An Exposure System for Variable Electromagnetic-Field Orientation Electrophysiological Studies

JOSEPH D. FORSTER, MEMBER, IEEE, FRANK S. BARNES, FELLOW, IEEE, HOWARD WACHTEL, RONALD R. BOWMAN, JAMES W. FRAZER, AND RICH CHALKER

Abstract—**A TEM system for exposing isolated nerve cells at 2 GHz is described. The system allows for monitoring of transmembrane potentials by means of microelectrodes and variation of the angle between the electric-field vector and the cell. An *S*-parameter characterization of the system is included along with temperature profile measurements for the energy distribution within the exposure chamber. Additional data on the transient electrical characteristics of microelectrodes upon exposure to microwave pulses in this system are included along with a few examples of the response of *Aplysia* pacemaker neurons to microwave fields.**

Key Words: **Microwave; Nerve Cells; Cell Measurement Systems.**

I. Introduction

A VALUABLE APPROACH in the study of the effects of microwaves on biological materials is to isolate a tissue so the effects on various biological feedback systems are minimized and the basic changes in the properties of individual cells can be studied and related directly to dosimetry. A coaxial system feeding a TEM line was chosen for the purpose of obtaining a broad-band system with a well-defined electromagnetic-field characterization [1]–[3]. The advantage of this system, which is shown in Figs. 1 and 2, is that the sides of the stripline of the TEM cell can contain slots large enough to allow for the mounting of isolated tissue samples on a plastic post which may be independently cooled. In addition, microelectrode probes are inserted into the cell at right angles to the electric field. This orientation minimizes the interaction between the RF field and the microelectrode probe. At the same time, it allows for independent control of the position of the cell and microelectrode with respect to the RF field. The TEM cell may be rotated on its base around the tissue sample, which is mounted on a fixed post. These slots also allow for the insertion of a high-impedance temperature probe (Vitek) at right angles to the electric field, for measurements of the rate of energy disposition into the cell sample.

The system has been characterized by measurement of the *S*-parameters and the rate of temperature rise as a function of position in the sample holder, and for rotation of the incident *E* field with respect to the sample holder. The field distributions and thermal characterizations show a consistent response which permits reasonable predictions to be made about the average field strengths and current densities in the cell preparations of interest for biological system studies. This system has been used primarily in studies of isolated *Aplysia* neurons, but it is applicable to a variety of situations in which small tissue samples need to be studied electrophysiologically.

Manuscript received September 7, 1984; revised March 18, 1985. This work was supported in part by ONR, under Contract N00014-81-K-0387.

J. D. Forster is with the Fonar Corporation, 110 Marcus Drive, Melville, NY 11747.

F. S. Barnes and H. Wachtel are with the Department of Electrical and Computer Engineering, University of Colorado, Campus Box 425, Boulder, CO 80309.

R. R. Bowman is with Vitek, Sentinal Rock Lane, Boulder, CO 80301.

J. W. Frazer is with UTSCC-M.D. Anderson Hospital, Section of Experimental Surgery, Box 17, 6723 Bertner Avenue, Houston, TX 77030.

R. Chalker is with the University of Colorado Health Science Center, 4200 E. Ninth Avenue, Denver, CO 80262.

II. Detailed Description of the Exposure System

The basic system is designed for matching the TEM section to a 50-Ω coaxial line in the frequency range from ~ 500 MHz to 2.45 GHz. The dimensions for the TEM cell and the holder for the cells are given in Fig. 2. These dimensions were picked primarily to allow sufficient room in the holder to anchor a neural ganglion (from the marine mollusk *Aplysia*) in a reasonable way, and secondarily, for the height of the TEM cell to be large enough to provide a relatively uniform expanse for the fields in its vicinity. The length of the TEM cell was chosen so that upon the application of a short at the output end, the peak of the standing wave is approximately centered on the cell holder at 2.45 GHz, as per the design of Wachtel *et al.* [1]. At lower frequencies, this maximum shifts towards the generator and the position of the short must be adjusted. The foregoing dimensions yield an impedance very close to 50 Ω while minimizing mismatches at transitions between it and the coaxial line. A still better match could be obtained by tapering the transition from the coaxial cable to the slotted section; however, for our application, this did not prove to be necessary.

The post that holds the tissue consists of two concentric plastic tubes with an H-shaped cap as shown in Fig. 1. This configuration serves two functions. The first is to allow cooling with distilled water which circulates close to the cell preparation, giving a relatively low thermal time con-

0018-9480/85/0800-0674$01.00 ©1985 IEEE

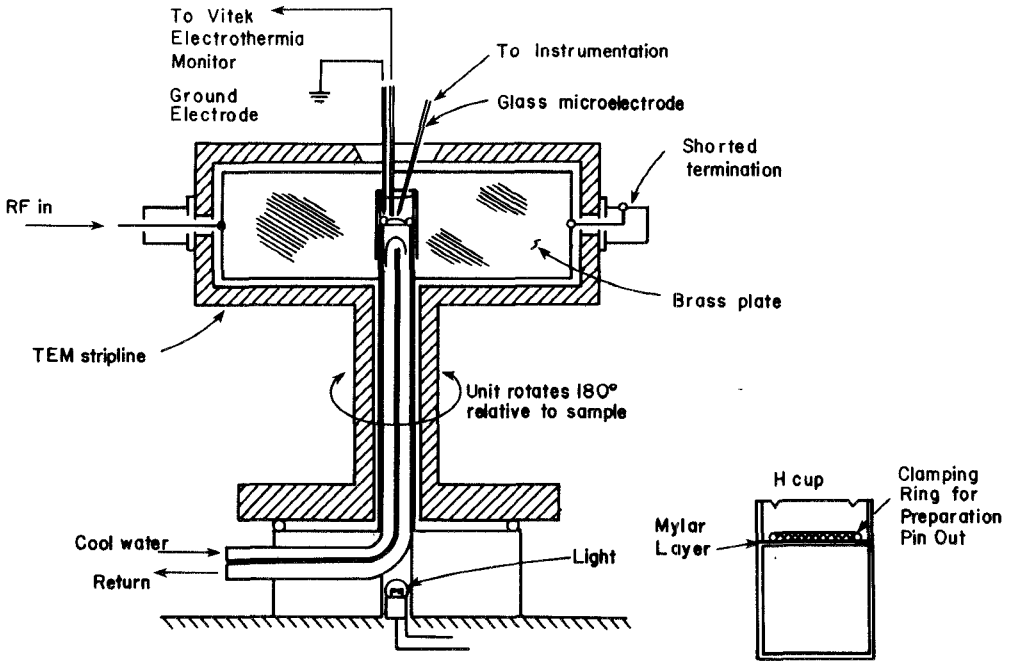

Fig. 1. Cutaway diagram of TEM cell.

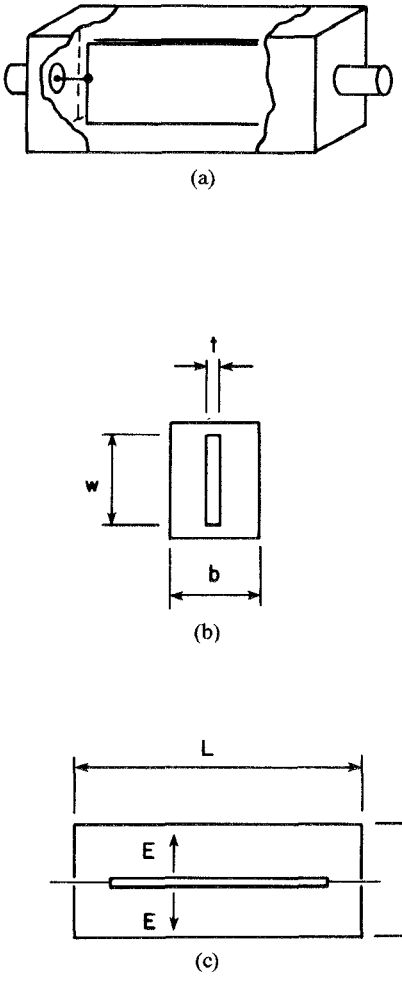

Fig. 2. (a) Cutaway diagram of stripline. (b) Cross-sectional view of stripline with dimension labels. (c) Top view of stripline with dimension labels. $W = 4.0$ cm, $t = 0.318$ mm, $b = 3.25$ cm, $L = 9.18$ cm.

stant of approximately 30 s (compared with an uncooled time constant of almost 20 min). In order to get this short time constant, the top of the post is machined to approximately 1 mm thick and the cup which is seated on it has a base which is formed from a thin Mylar sheet (0.16 mil). The post also includes a lamp for transilluminating the ganglion so that it can be viewed from the top side. This enables the experimenter to locate microelectrodes in a given cell and to orient the ganglion precisely along a reproducible set of axes.

III. Microwave Coupling

For isolated cell exposures, the microwave system as shown in Fig. 3 contains a generator which will provide up to 100 W of incident power into the stripline. The attenuator in the system yields nominal power reductions of up to 60 dB (which is useful for finding threshold values associated with changes in the cell characteristics). An isolator prevents feedback from the load to the generator, and both the incident and reflected powers are monitored through a bidirectional coupler. Exposure times are controlled by a coaxial switch that allows power to be directed into a dummy load except during experimental exposures. In normal operation, the stripline is terminated in a short so that the incident and reflected waves incident on a tissue are similar in size. The standing wave yields a more uniform energy deposition in the cell system than would result from a single traveling wave terminated in a matched load.

In order to further characterize this system, the TEM line was disconnected from its standard driving system and connected to an HP network analyzer Model No. 8410B, which allowed for direct measurements of the *S*-parameters. The basic characterization resulting from this evalua-

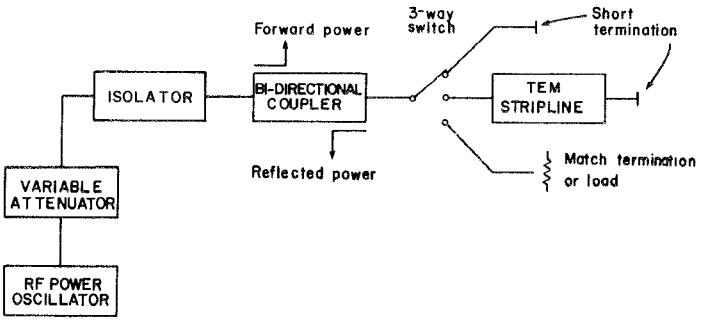

Fig. 3. Block diagram of microwave delivery system.

TABLE I
CHARACTERIZATION OF STRIPLINE AT 2 GHz

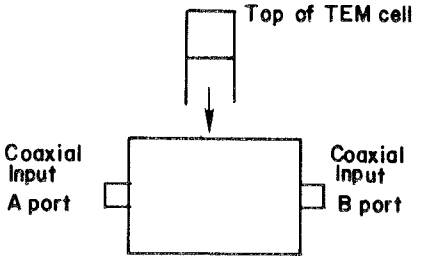

$\lvert S_{11}\rvert^2 =$	$\lvert S_{22}\rvert^2 =$	$\lvert S_{21}\rvert^2 =$	$\lvert S_{12}\rvert^2 =$	A port Measurements
.05	.04	.79	.79	Empty Cavity
.05	.05	.45	.45	Cavity and Post
.08	.08	.35	.40	Cavity, Post and Chamber with Saltwater

TABLE II
PORT A CONNECTED TO TEM CELL TERMINATED IN A SHORT;
PORT B CONNECTED TO ELECTRODE AT 2 GHz

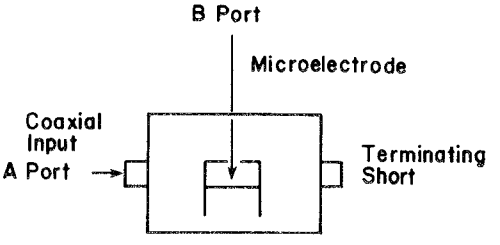

Results	
$\lvert S_{11}\rvert^2$	.71
$\lvert S_{12}\rvert^2$	3.2×10^{-5}
$\lvert S_{21}\rvert^2$	3.2×10^{-5}
$\lvert S_{22}\rvert^2$	.58

tion at 2 GHz is shown in Table I. The accuracy of the measurement system was ± 0.05 dB in magnitude and $\pm 2°$ in phase. These data show the characteristics of the stripline by itself, the effect of the water-filled post both with and without a sample, in perturbing the system, and the effect of the microelectrode.

Additional data in Table II depict the transmission characteristics at 2 GHz where the S-parameters are measured through the microelectrode. These data are significant because the TEM cell is relatively well-matched and the perturbations due to the water-filled post and cell sample are moderate. Furthermore, the data on transmission through the microelectrode show that the coupling coefficient for power through the microelectrode is typically less than one part in 10^5.

IV. Temperature Rise Rate and Profile Measurements

In order to corroborate our calculated dosimetry and to make measurements of the uniformity of the energy deposited in the tissue chamber, temperature-rise measurements were made with a high-impedance Vitek probe. The probe was also inserted at right angles to the electric field to minimize its effects on the field. The Vitek probe allows for measurements of the rate of rise of the temperature due to the absorption microwave power with an accuracy of $\pm 0.1°C$ and a spatial resolution of ~ 0.5 mm. The diameter of the Vitek probe is about 1 mm and its position is controlled with a micromanipulator. Any fluctuations due to inhomogeneity within the tissue were not resolvable. The

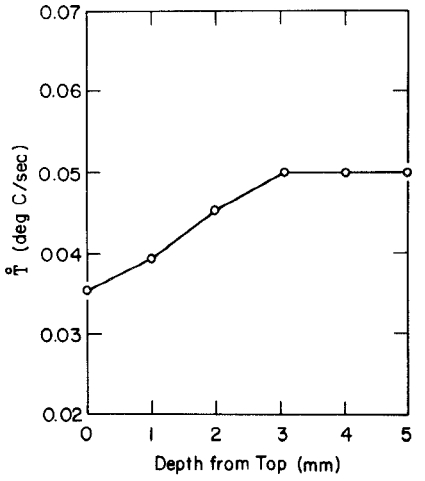

Fig. 4. Variations in the rate of temperature rise as a function of depth from top of the liquid in chamber, 0.5-cc saltwater, probe in center of chamber.

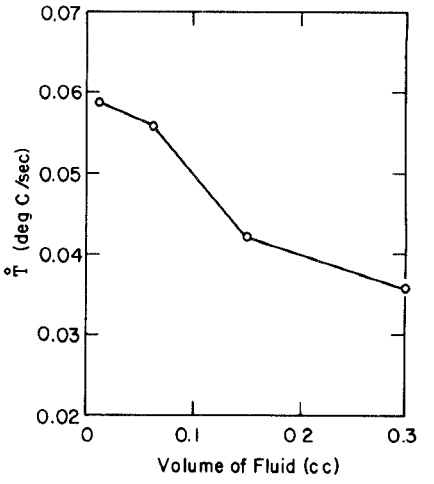

Fig. 6. Variations in rate of temperature rise as a function of volume of fluid in sample chamber, 0.5-cc saltwater at constant center location.

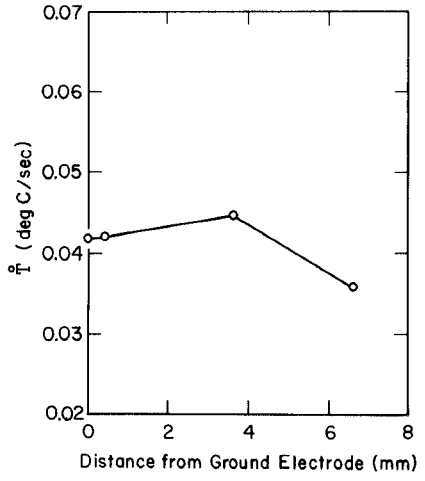

Fig. 5. Variations in rate of temperature rise as probe is varied from ground electrode at constant depth, 0.5-cc saltwater.

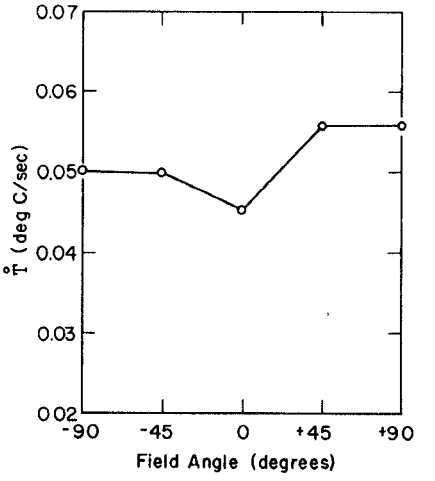

Fig. 7. Variations in rate of temperature rise as a function of field angle, 0.5-cc saltwater, probe at constant depth, center of chamber.

specific absorption rate (SAR) in a given portion of the tissue sample volume is closely proportional to the rate of the temperature rise since heat dissipation is relatively slow in the uncooled case. Plots of these temperature rates of rise as functions of position in the cell sample are shown in Figs. 4–6. At the center of the sample, temperature rates of rise from top to bottom of the sample varied by 0.015°C/s. This represents approximately a 30-percent variation from top to bottom. However, in the region where the cells are located ~3 mm below the surface, variations in temperature rate of rise were not measurable. Variations in the rate of rise of temperature as the probe is moved away from the center of the sample are about 10 percent over the first 4 mm. At the edges of the cup, the temperature rate of rise decreases by about 30 percent.

Putting an additional probe in the field makes essentially no difference in the temperature rate of rise (less than 10 percent). Increasing the volume of the fluid in the sample holder decreases the rate of temperature rise in an approximately linear way. More significantly, as the angle of field is rotated with respect to the sample (see Fig. 7), less than 10-percent variation in the rate of temperature rise occurs over a 180° rotation. The variation with angle for the water samples is probably the result of a slight tilt of the center post supporting the sample with respect to the stripline.

V. Characterization of the Microelectrodes

The microelectrodes are pulled to tip diameters of less than 1 μm using a standard electrode puller. Connection to this microelectrode is made with a silver chloride wire located outside the microwave field. To further reduce the disturbance of the microwave field by the electrode probing system, the ground electrode is made through a salt bridge using a larger diameter, low-impedance pipette (typically 100 kΩ), which is also located at the edge of the cup nearest the outside metal wall of the TEM cell and as close as possible to one of the RF ground plates. The ground electrode contains ~10-percent agar plus artificial sea water, which is the same solution as that used to bathe

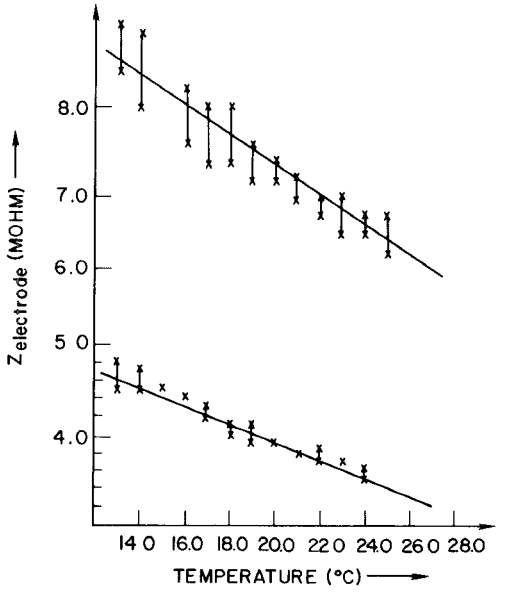

Fig. 8. Electrode impedance versus temperature.

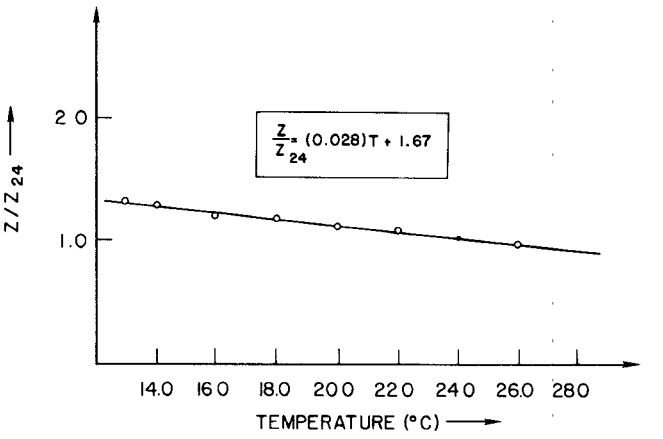

Fig. 9. Electrode impedance (normalized to impedance at 24°C) versus temperature.

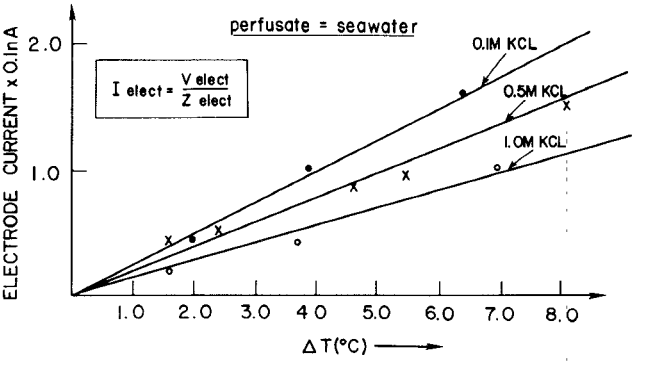

Fig. 10. The equivalent electrode current versus ΔT for three different electrode concentrations, where ΔI is calculated from the measured ΔV divided by the initial electrode resistance.

the preparation. Again, a silver chloride wire located outside the RF field is used to connect to the circuit ground bus.

In making intercellular microelectrode measurements under varying thermal environments, it is necessary to be aware of how the electrical characteristics of the microelectrodes change during the course of the measurements. A number of experiments are performed in order to determine:

1) the microelectrode impedance behavior as a function of temperature,
2) the magnitude and significance of equivalent electrode current contributed by the microelectrode under temperature excursions,
3) the effect of varying KCl concentrations in the microelectrodes on 2),
4) the microelectrode behavior as a function of the rate at which the temperature is changed ($\dot{T}$).

For these experiments, the microelectrodes are made of 2-mm capillary tubing using a standard electrode puller. After pulling and cooling, the electrodes are placed with blunt ends in ~3 cm of 0.5-M KCl electrolyte solution until the tips are filled by capillary action. They are then back-filled the rest of the way with the same 0.5-M KCl solution using a specially adapted syringe. The concentration of the electrolyte and the setting on the puller are such that the electrode impedance is in the range of 2 to 20 MΩ. After filling, the electrodes are checked for tip breakage and/or excessive bubbles under a microscope. Any showing defects are rejected.

A microelectrode is then placed in the micromanipulator and the system is set up for intracellular measurements but without a ganglion in the preparation chamber. The perfusion system (perfusate–sea water) is activated and a room-temperature baseline established. A known amount ($\approx$1 nA) of amplifier-injected current is passed through the electrode and the response recorded on the chart recorder. The baseline perfusion temperature is then lowered and the measurement repeated for a range of temperatures between 13° and 26°C on two separate electrodes. The calculated impedance is shown as a function of temperature in Fig. 8. The curves in Fig. 8 are normalized to their impedance at 24°C and plotted in Fig. 9. This curve may be used to determine impedance changes as a function of temperature for any electrode with 0.5-M KCl and between 2 and 20 MΩ.

In other experiments with the same initial protocol, a microelectrode is subjected to perfusion-produced temperature "pulses" and its response is recorded on the chart recorder. The electrode potential shifts as a function of temperature excursion are then converted to equivalent electrode current by dividing the measured electrode voltage shift by the initial electrode resistance. The results are plotted as a function of the size of the temperature excursion (ΔT) in Fig. 10. They indicate an equivalent electrode injected current of less than 0.01 nA per 1° change in electrode temperature. This current is small enough that, under most circumstances, it has very little effect on the

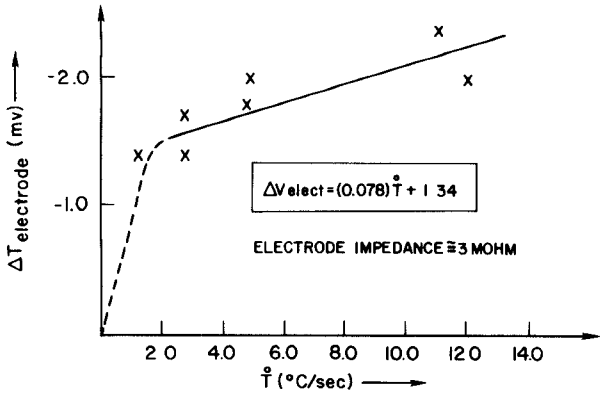

Fig. 11. Electrode potential shift versus T at 19°C.

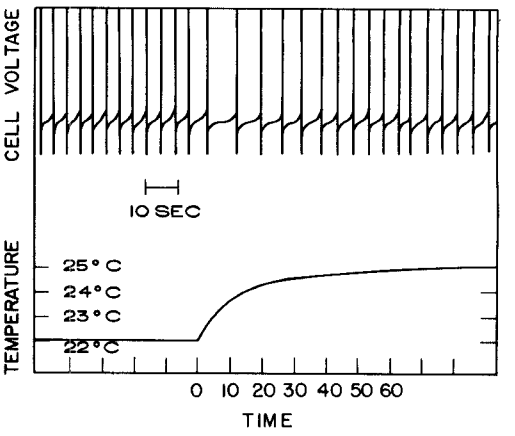

Fig. 12. The firing rate change as the result of the application of 15 W at 2.45 GHz. The absorbed power $P_a = 0.3$ W/cm^3, $T_{max} = 0.14$°C/s, and $\Delta T = 3$°C.

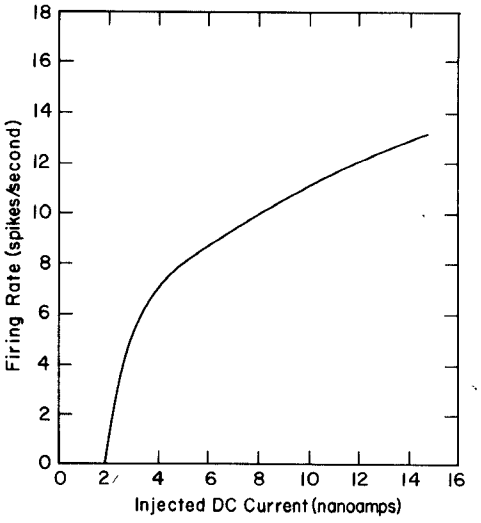

Fig. 13. Changes in the firing rate of a pacemaker cell as determined by injecting current step and noting the initial shift in the interspike interval.

firing rate of the pacemaker nerve cells. However, it can have a significant effect on the apparent voltage shift, seen when measuring the response of a silent cell. This is because the typical membrane resistance for a silent cell is ~1 MΩ, and thus the temperature-induced change in voltage as measured across the electrode plus the membrane can be 4 to 8 times that produced by the membrane alone. Fortunately, the time constants for the voltage from the microelectrode is 1.25 s and that for the membrane plus electrode is 3.25 s. Thus, the effect of the microelectrode can be subtracted out.

The final microelectrode characterization includes a determination of the microelectrode behavior as a function of the rate at which its temperature changes with time ($\dot{T}$). A microelectrode is subject to a series of "equal energy" microwave pulses, all of different lengths (0.2 to 5 s) but all raising the temperature of the perfusate (and electrode) by ~ 3.5°C. The electrode potential shifts in response to these pulses are recorded on a chart recorder. The magnitude of the maximum shift is plotted as a function of the rate at which the temperature was changed ($\dot{T}$) in Fig. 11. $\dot{T}$ is determined by dividing the extent of temperature excursion by the length of the microwave pulse. The dashed portion of Fig. 11 is drawn in from an assumed origin. The apparent microelectrode $\dot{T}$ sensitivity indicated in Fig. 11 is surprising but may be explained by the fact that there exists a potential barrier between the perfusate medium and the 0.5-M KCl electrode solution. The ion-concentration difference between the two regions is related by the Nernst equation [4] so that $C_1 = C_2 \exp[q\phi/\zeta KT]$ and a current $I \sim \Delta T/T$ is generated by a temperature pulse ΔT [5]. C_1 and C_2 are concentrations, q is the ion charge, K is the Boltzmann constant, ϕ is the potential, ζ is a parameter on the order of unity, and T is the temperature.

VI. Some Examples of the System's Use: Microwave Effects on *Aplysia* Pacemaker Neurons

The results in Fig. 12 show the change in firing rate for a typical pacemaker cell (taken from the ganglion of an *Aplysia*) after turning on a CW microwave signal leading to a rise of ~ 2°C in 15 s. The total temperature rise is determined by the balance between the absorbed microwave power and cooling through the plastic post, with a thermal relaxation time of about 30 s. Following application of the microwave signal, the cell first slows down, and then accelerates. A similar change in firing rate can be obtained by injecting a hyperpolarizing current (which makes the interior of the cell more negative) into the cell through the sensing microelectrode [6]. The amount of pulsed current required to increase the firing rate of a typical cell is shown in Fig. 13 [7]. The amount of current required to get a given change in the firing rate is very nonlinear, and is strongly dependent on how far the natural operating point for the cell is displaced from the cutoff where the cell ceases to oscillate.

VII. Conclusions

The exposure system described allows for relatively uniform exposure of isolated neural tissue at 2.45 GHz and nearby frequencies. The recording microelectrode is shown

to be sensitive to both temperature and the rate of temperature rise. Temperature rate of rise measurements as a function of the angle between the electric field and the tissue sample holder, and depth, show that a relatively uniform power density is being deposited in the cell sample with the variations in the SAR of less than 10 percent. We believe that this system is well suited for exposing a variety of tissues to RF fields, the direction of which can be varied while responses are monitored with microelectrodes. Additionally, some sample results are given which show that changes in the firing rate of pacemaker cells taken from the ganglion of an *Aplysia* are induced by microwave pulses.

REFERENCES

[1] H. Wachtel, R. Seaman, and W. Joines, "Effects of low-intensity microwaves on isolated neurons," *Ann. NY Acad. Sci.*, vol. 247, pp. 46–62, 1975.

[2] M. L. Crawford, "Generation of standard EM fields using TEM transmission cells," *IEEE Trans. Electromagn. Compat.*, vol. EMC-16, pp. 189–195, 1975.

[3] S. V. Marshall, R. F. Brown, C. W. Hughes, and P. V. Marshall, "Environmentally controlled exposure system for irradiation of mice at frequencies below 500 MHz," in *IEEE Int. Symp. Electromagn. Compat.*, 1981, pp. 99–104.

[4] R. J. MacGregor and E. R. Lewis, *Neural Modeling.* New York: Plenum Press, 1977, chs. 6, 7.

[5] F. S. Barnes, "Cell membrane temperature rate sensitivity predicted from the Nernst equation," *BEMS*, vol. 5, pp. 113–115, 1983.

[6] D. O. Carpenter, "Temperature effects on pacemaker generation membrane potential and critical firing threshold in *Aplysia* neurons," *J. Gen. Phys.*, vol. 50, no. 6, part I, pp. 1469–1484, 1967.

[7] J. Forster, "Nonlinear microwave bioeffects on isolated neurons of *Aplysia*," Masters thesis, Dept. Elec. Eng., Univ. of Colorado, 1981.

Joseph D. Forster (S'75–M'81) received the B.S. degree in engineering science in 1978 from New Jersey Institute of Technology, Newark, NJ, and the M.S.E.E. degree in 1981 from the University of Colorado in Boulder, CO.

From 1981 to 1983, he was a Staff Engineer at Baylor College of Medicine, where he became involved with NMR studies of biological systems and NMR whole body imaging. In 1983, he joined Fonar Corporation, Melville, NY, where he became Project Engineer for the Fonar Mobile NMR and is now Assistant to the Vice President of Operations in Manufacturing.

Mr. Forster is a member of Sigma Xi and the Bioelectromagnetic Society.

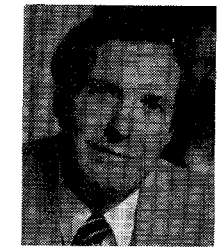

Frank Barnes (S'54–M'58–F'70) received the B.S. degree from Princeton in 1954, and the M.S. and Ph.D. degrees from Stanford in 1955 and 1958, respectively.

From 1957 to 1958, he taught at the College of Engineering in Baghdad, Iraq, on a Fulbright. In 1958, he joined the Colorado Research Corp. as a Research Associate. He joined the Department of Electrical Engineering at the University of Colorado, Boulder, in 1959, where he is a Professor. He served as Department Chairman from 1964 to 1980.

Dr. Barnes has been involved in the study of lasers, microwave devices, and their applications to biological materials. He is a fellow of AAAS and has received the Curtis McGraw Award for Research from ASEE in 1965. He is also a member of the American Physical Society and the Biolelectromagnetic Society.

Howard Wachtel, photograph and biography unavailable at the time of publication.

Ronald R. Bowman, photograph and biography unavailable at the time of publication.

James W. Frazer received a degree in basic medical sciences (State University of New York, College of Medicine, Syracuse, NY, 1965) with expertise in biochemistry, pharmacology, physiology, and biophysics. His interests for many years have been in examination of the electromagnetic behavior of biomacromolecular systems with experimental approaches utilizing optical spectroscopy (absorbance and light scattering) resonance spectroscopies, nuclear magnetic resonance (NMR), electron spin resonance (ESR), resonant Raman spectroscopy, Raman spectroscopy, and a variety of EM-wave applicators to biological systems. His present efforts include NMR examination of tumor cells and the use of electromagnetically induced hyperthermia in tumor treatment.

Rich Chalker, photograph and biography unavailable at the time of publication.